AFRL-RQ-WP-TR-2022-0036

INVESTIGATION OF HYBRID POWERTRAINS FOR SMALL UNMANNED AIRCRAFT SYSTEMS

Stephen Akwaboa
Southern University
Department of Mechanical Engineering

JANUARY 2022

AIR FORCE RESEARCH LABORATORY
AEROSPACE SYSTEMS DIRECTORATE
WRIGHT-PATTERSON AIR FORCE BASE, OH 45433-7542
AIR FORCE MATERIEL COMMAND
UNITED STATES AIR FORCE

REPORT DOCUMENTATION PAGE

PLEASE DO NOT RETURN YOUR FORM TO THE ABOVE ORGANIZATION.

1. REPORT DATE	2. REPORT TYPE	3. DATES COVERED	
		START DATE	END DATE
20-01-2022	Thesis	20-09-2018	27-12-2021

4. TITLE AND SUBTITLE

INVESTIGATION OF HYBRID POWERTRAINS FOR SMALL UNMANNED AIRCRAFT SYSTEMS

5a. CONTRACT NUMBER	5b. GRANT NUMBER	5c. PROGRAM ELEMENT NUMBER
FA8650-18-2-2232	FOA-AFRL-RQKP-2017-0001	62203F
5d. PROJECT NUMBER	**5e. TASK NUMBER**	**5f. WORK UNIT NUMBER**
6206WP		Q239

6. AUTHOR(S)

Stephen Akwaboa

7. PERFORMING ORGANIZATION NAME(S) AND ADDRESS(ES)

Southern University
Department of Mechnical Engineering
B A Little Dr.
Baton Rouge, LA 70813-0001

8. PERFORMING ORGANIZATION REPORT NUMBER

9. SPONSORING/MONITORING AGENCY NAME(S) AND ADDRESS(ES)	10. SPONSOR/MONITOR'S ACRONYM(S)	11. SPONSOR/MONITOR'S REPORT NUMBER(S)
Air Force Research Laboratory Aerospace Systems Directorate Wright-Patterson Air Force Base, OH 45433-7542 Air Force Materiel Command	AFRL/RQQE	AFRL-RQ-WP-TR-2022-0036

12. DISTRIBUTION/AVAILABILITY STATEMENT

DISTRIBUTION STATEMENT A. Approved for public release. Distribution is unlimited.

13. SUPPLEMENTARY NOTES

PA Clearance Number: (Number)

14. ABSTRACT

The overarching goal of this work was to investigate hybrid powertrains for propulsion of small unmanned aircraft systems. The specific task objectives were: 1.) Development of computational tools for hybrid powertrain sizing and design; 2.) Performance measurement of powertrain components at steady-state and transient conditions; 3.) Evaluation of hybrid configurations using metrics most relevant to small unmanned aircraft systems; 4.) Development and bench testing of a hybrid powertrain with associated controllers; 5.) Integration of the powertrain and controller with a suitable airframe. The demand on unmanned aerial vehicles (UAVs) for execution of combat, surveillance, and reconnaissance missions has increased greatly across the world, henceforth modeling and simulation of aircraft systems are necessary to eliminate unnecessary costs. In this project, a longitudinal three degree of freedom aircraft model was developed and its performance monitored via two basic control inputs – the throttle position and elevator deflection. The model utilizes the nonlinear longitudinal equation of motion considered for aircraft designs. The nonlinear aircraft model is further trimmed to obtain the operating points necessary for the linearization. Trimming and linearization of the model were achieved by using a linear analysis tool available in MATLAB/Simulink. Using the Ziegler Nichol control scheme the corresponding gains necessary for stabilizing the system are developed. To further validate the model, an open source aircraft data (Aerosonde) was used. The performance of the aircraft was evaluated by comparing the non-linearized and linearized model results.

15. SUBJECT TERMS

UAV, hybrid powertrain, modeling, simulation, analysis

16. SECURITY CLASSIFICATION OF:			17. LIMITATION OF ABSTRACT	18. NUMBER OF PAGES
a. REPORT	b. ABSTRACT	C. THIS PAGE		
Unclassified	Unclassified	Unclassified	SAR	33

19a. NAME OF RESPONSIBLE PERSON	19b. PHONE NUMBER *(Include area code)*
Chad N. Miller	(937) 255-4122

Investigation of Hybrid Powertrains for small Unmanned Aircraft Systems

Opportunity Number:FOA-AFRL-RQKP-2017-0001
: FA8650-18-2-2232

Final Report Prepared for AFRL

By

Stephen Akwaboa

Assistant Professor

Department of Mechanical Engineering

Southern University

Baton Rouge, LA 70813

January 20, 2022

Abstract

The overarching goal of this work is to investigate hybrid powertrains for propulsion of small unmanned aircraft systems. The period of performance is 2 years. The specific task objectives are:

- Development of computational tools for hybrid powertrain sizing and design
- Performance measurement of powertrain components at steady-state and transient conditions
- Evaluation of hybrid configurations using metrics most relevant to small unmanned aircraft systems
- Development and bench testing of a hybrid powertrain with associated controllers
- Integration of the powertrain and controller with a suitable airframe

The demand on Unmanned Aerial Vehicles (UAVs) for execution of combat, surveillance and reconnaissance missions have increased greatly across the world henceforth modeling and simulation of aircraft systems are necessary to eliminate unnecessary costs. In this project, a longitudinal three degree of freedom aircraft model is developed and its performance monitored via two basic control inputs – the throttle position and elevator deflection. The model utilizes the nonlinear longitudinal equation of motion considered for aircraft designs. The nonlinear aircraft model is further trimmed to obtain the operating points necessary for the linearization. Trimming and linearization of the model were achieved by using a linear analysis tool available in Matlab/Simulink. Using the Ziegler Nichol control scheme the corresponding gains necessary for stabilizing the system are developed. To further validate the model, an open source aircraft data (Aerosonde) is used. The performance of the aircraft is evaluated by comparing the non-linearized and linearized model results.

2. Acknowledgement

This work was sponsored by a grant from Air Force Research Laboratory (AFRL) with grant number FOA-AFRL-RQKP-2017-0001**.** We are particularly grateful to the all the AFRL collaborators who worked with us (Chad Miller, Thomas Howell, Michael Rottmayer) on the project. Their assistance in the tag-up meetings was greatly appreciated.

3. Table of Contents

4. List of Tables

5. List of Figures

6. Introduction

This project is aimed at analyzing hybrid powertrains suitable for propulsion of small unmanned aircraft systems (SUAS). For SUAS applications, validated sizing and design tools are required to compare different hybrid powertrain layouts. While previous studies have considered such tools, they lack reliable performance data for components such as engines, generators, and propellers, at steady state and transient conditions. Scaling of performance data with size is another key unknown. The impact of commercial-off-the-shelf technologies such as electronic fuel injection and variable pitch propellers on powertrain performance needs further investigation. Finally, practical considerations such as integration into a suitable airframe and development of powertrain controllers requires further research. This project aims to utilize computational and experimental methods to address the issues mentioned above and to identify, develop, and test a candidate hybrid powertrain.

This work is sponsored by the Air Force Research Laboratory (AFRL) and the work loads were executed by three main universities including Southern University and A&M College (SUBR), Louisiana State University (LSU) and Oregon State University (OSU). The assigned tasked are presented in the flow chart below.

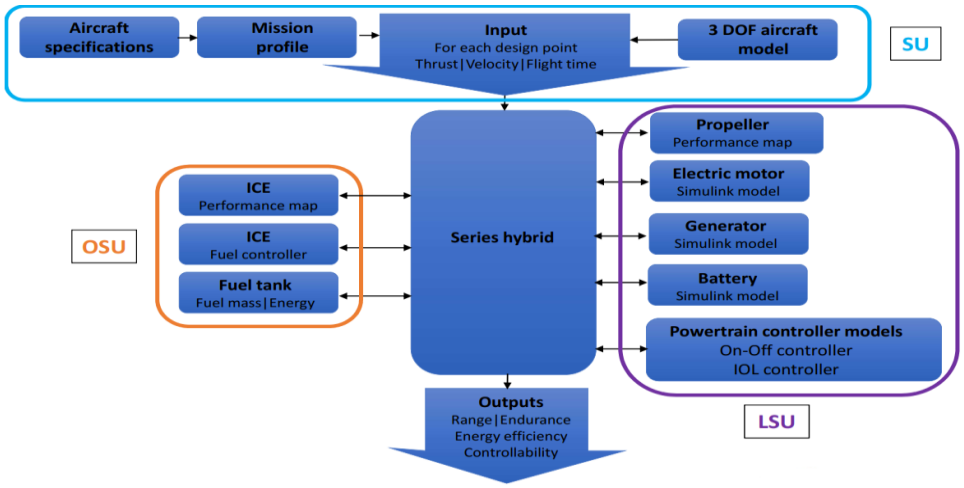

Figure 1: Work load Allocation

Simulation of physical systems from the inception of engineering has been a technique adopted in predicting a system's behavior with governing equations. In fact a lot of benefits can be attributed to aircraft modeling and simulation. Aircraft systems performance can be simulated prior to building actual aircraft systems and this in many ways save industries unnecessary costs. Through aircraft simulation the designer is privileged to access the system performance using gathered data during real flight. Additionally, aircraft system performance can be monitored using simulators such as flight gear and xplane. In this thesis a longitudinal (three degree of freedom, 3DOF) dynamic model of an aircraft will be developed. The aircraft stability analysis in the phugoid (long period mode) and short period mode are addressed. In aircraft modeling and simulation it is pertinent to ensure both static and dynamic modeling requirements are achieved (A. E. Ahmed et al., 2015). Conventional aircrafts which are dynamically stable are statically stable henceforth it is crucial to ensure an aircraft model is dynamically stable. Dynamic modeling considers the trimming and linearization of the aircraft model which facilitate control analysis of the entire aircraft system. The model is structured to allow elevator, throttle inputs as well as the effect of wind. The control

analysis is incorporated to enable the system achieve its system requirements. The Aerosin aerospace blockset was used in building a 3dof UAV. As part of the design process Aerosonde UAV mission profile was considered.

7. Objectives

The main objectives for Southern University's portion of the project are listed below:

- Simulation of Aircraft Dynamics (Longitudinal Model) for unmanned Aerial Vehicles
- Stabilize aircraft in long period (phugoid mode) and short period mode using control techniques (Ziegler Nichols heuristic approach for PID gains estimation)
- Analyze the Aircraft Dynamics time history of the various parameters in the longitudinal mode (u, w, q, theta, h, AOA).
- Investigate the effect of wind on the aircraft's propulsion system using the Dryden Turbulence model available in Matlab.

8. Equation of Motion

The aircraft equation of motion is derived from the well-known Newton Second Law of motion, $F = ma$ where **F** is the total force acting on the aircraft, **m** is total mass of the aircraft and **a** is the total acceleration acting on the aircraft. The derivation of aircraft equation of motion is detailed in flight dynamics textbooks, typically, Aircraft Dynamics and from Modeling to Simulation by Marcello R. Napolitano. In his textbook he details relevant equation motion for aircraft modeling and categorizes them into Conservation of Linear and Angular momentum equations respectively. He further uses the concept of rotation between inertial and rotating bodies to perform between rigid bodies. The axes system used in his textbook is shown in Figure 2.

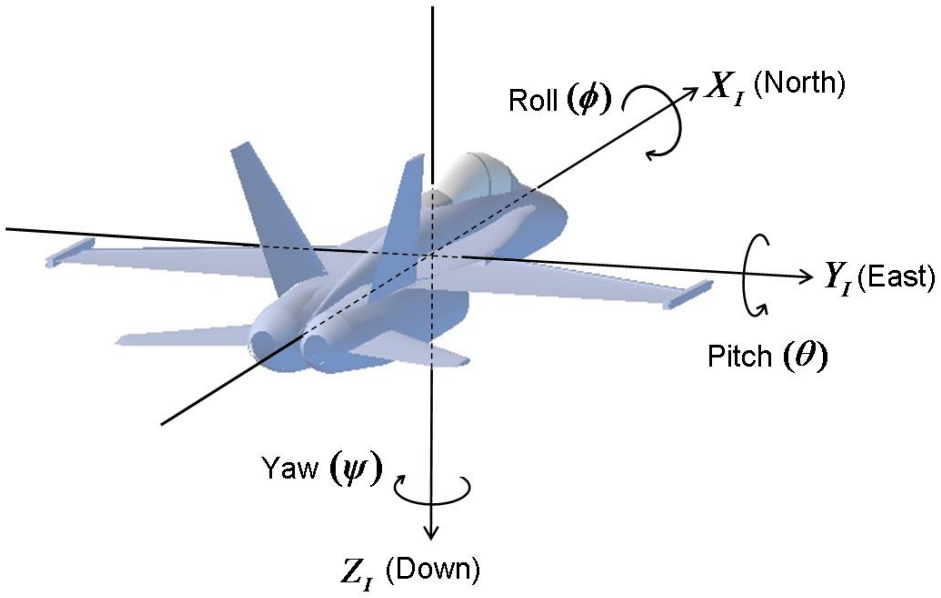

Figure 2: Aircraft Axes System

Upon applying the assumptions listed by Napolitano above, equation the 2.16 to2.21 are obtained

8.1 Conservation of Linear Momentum Equation of Motion

$$m(\dot{U} - VR + WQ) = -mg\sin\theta + F_{A_x} + F_{T_x} \quad 2.16$$

$$m(\dot{V} - UR + WP) = -mg\sin\phi\cos\theta + F_{A_y} + F_{T_y} \quad 2.17$$

$$m(\dot{W} - UQ + VP) = mg\cos\phi\cos\theta + F_{A_Z} + F_{T_Z} \quad 2.18$$

8.2 Conservation of Angular Momentum Equation of Motion

$$I_{xx}\dot{P} - I_{xz}(\dot{R} + PQ) + (I_{xz} - I_{yy})RQ = L_A + L_T \quad 2.19$$

$$I_{yy}\dot{Q} - I_{xz}(P^2 + R^2) + (I_{xx} - I_{zz})PR = M_A + M_T \quad 2.20$$

$$I_{zz}\dot{R} - I_{xz}\dot{P} + (I_{yy} - I_{xx})PQ + I_{xz}RQ = N_A + N_T \quad 2.21$$

Simplifying equation 2.16 to 2.19 above equation 2.22 to 2.27 are obtained. U V W are velocity components in the X, Y and Z directions; P, Q, and W are angular velocity along roll (ϕ), pitch (θ) and yaw (Ψ) axes; D, Y and L are the aerodynamic drag, side force and lift; L_A, M_A and N_A are the aerodynamic moments about the roll, pitch and yaw exes respectively.

$$\dot{U} = VR - WQ - g\sin\theta + \frac{1}{m}(-D + T\cos\alpha) \quad 2.22$$

$$\dot{V} = -UR + WP + g\sin\phi\cos\theta + \frac{1}{m}(Y + Tcos\alpha sin\beta) \quad 2.23$$

$$\dot{W} = UQ - VP + g\cos\phi\cos\theta + \frac{1}{m}(-L - Tsin\alpha) \quad 2.24$$

$$\dot{P} = \frac{I_{xz}}{I_{xx}}(\dot{R} + PQ) - \frac{(I_{xz} - I_{yy})}{I_{xx}}RQ + \frac{L_A + L_T}{I_{xx}} \quad 2.25$$

$$\dot{Q} = \frac{I_{xz}}{I_{yy}}(P^2 + R^2) - \frac{(I_{xx} - I_{xx})}{I_{yy}}PR + \frac{M_A + M_T}{I_{yy}} \quad 2.26$$

$$\dot{R} = \frac{I_{xz}}{I_{zz}}\dot{P} + \frac{(I_{yy} - I_{xx})}{I_{zz}}PQ - \frac{I_{xz}}{I_{zz}}RQ + \frac{N_A + N_T}{I_{zz}} \quad 2.27$$

The aerodynamic forces (lift, drag and side force) and moments (roll, pitch and yaw) are estimated using the equations 2.28 to2.33 below;

C, S, b and, $\bar{q}$ are the mean aerodynamic chord, wing reference area, wing span and dynamic pressure respectively.

$$\text{Drag}, D = \bar{q}SC_D \quad 2.28$$

$$\text{Sideforce}, Y = \bar{q}SC_y \quad 2.29$$

$$\text{Lift}, L = \bar{q}SC_L \quad 2.30$$

$$\text{Roll}, L_A = \bar{q}SC_l b \quad 2.31$$

$$\text{Pitch}, M_A = \bar{q}SC_m c \quad 2.32$$

$$\text{Yaw}, N_A = \bar{q}SC_n b \quad 2.33$$

9. Problem Formulation and Methodology

This section presents a step by step method used in modeling a three degree of freedom (3DOF) aircraft model for unmanned aerial vehicle. The primary models include aerodynamics, international standard atmosphere model, total acceleration, propulsion, UAV inertia, total moment, wind model and equation of motion. Aerosonde UAV data was used in the validation of the aircraft model. The aircraft model implements the longitudinal equation of motion of an aircraft obtained in the body axes system. The main inputs are the ***throttle and elevator deflection***. The linear and angular accelerations are integrated upon solving the equation of motion to obtain the aircraft state variables including the linear velocity, pitch rate and pitch angle. Detail presentation of the aircraft formulation adopted is shown in Figure 3 below.

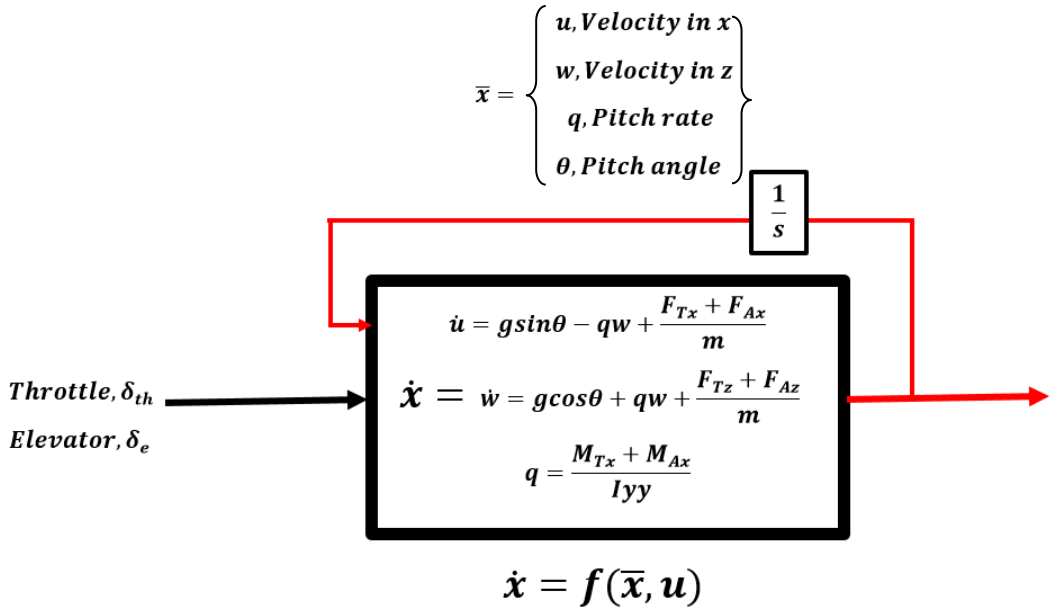

Figure 3. 3DOF Aircraft Equation of motion block diagram

9.1 Initialization inputs

In other to run the simulation, the aircraft model was initialized with the following set of values indicated in Table 1 below.

Table 1: Initialization Parameters

INPUT	
Throttle	50 %
Elevator Deflection	0.1 rad
OUTPUT	
Distance along x	0 m
Distance along z	0 m
Velocity in x, u	24 m/s
Velocity in z, w	0 m/s
Pitch angle, theta	0 rad
Pitch rate, q	0 rad/s

9.2 Steady State level flight

A steady state level flight was achieved by selecting a combination of state and control variables such that the translational and rotational acceleration are equal to zero. The general form of the equation used is represented by equation 3.35.

$$\dot{x} = f(x_o, u_o) = 0 \qquad 3.35$$

The model was trimmed by using the linear analysis tool available in matlab.

The linear time invariant (LTI) representing the aircraft for small perturbation about the reference trim condition was taken. The procedure adopted is presented below;

The general form of the equation of motion is represented by equation 3.36,

$$\dot{x} = f(x, u) \qquad 3.36$$

which can written implicitly as

$$\overline{0} = F(\dot{x}, x, u) \qquad 3.38$$

Applying Taylor's series expansion about the trimmed conditions to equation 3.38, equation 3.39 is obtained.

$$F(\eta) = F(\dot{x}_o x_o u_o) + \frac{\partial F(\dot{x}_o x_o u_o)}{\partial \dot{x}}(\dot{x} - \dot{x}_o) + \frac{\partial F(\dot{x}_o x_o u_o)}{\partial x}(x - x_o) + \frac{\partial F(\dot{x}_o x_o u_o)}{\partial u}(u - u_o) \qquad 3.39$$

where

$$\boldsymbol{\eta_0} = \begin{pmatrix} \dot{x}_o \\ x_o \\ u_o \end{pmatrix} \tag{3.40}$$

Considering the individual terms in equation 3.39 and finding their respective Jacobian matrix and evaluating at their respective trim values gives;

$$E = \frac{\partial F(\dot{x}_o x_o u_o)}{\partial \bar{x}} = \begin{bmatrix} \frac{\partial F_1}{\partial \dot{x}_1} & \frac{\partial F_1}{\partial \dot{x}_2} & \frac{\partial F_1}{\partial \dot{x}_n} \\ \frac{\partial F_2}{\partial \dot{x}_1} & \frac{\partial F_2}{\partial \dot{x}_2} & \frac{\partial F_2}{\partial \dot{x}_2} \\ \frac{\partial F_n}{\partial \dot{x}_n} & \frac{\partial F_n}{\partial \dot{x}_n} & \frac{\partial F_n}{\partial \dot{x}_n} \end{bmatrix}_{\substack{\dot{x}=\dot{x}_o \\ x=x_o \\ u=u_o}} \tag{3.41}$$

$$A' = \frac{\partial F(\dot{x}_o x_o u_o)}{\partial x} = \begin{bmatrix} \frac{\partial F_1}{\partial x_1} & \frac{\partial F_1}{\partial x_2} & \frac{\partial F_1}{\partial x_n} \\ \frac{\partial F_2}{\partial x_1} & \frac{\partial F_2}{\partial x_2} & \frac{\partial F_2}{\partial x_2} \\ \frac{\partial F_n}{\partial x_n} & \frac{\partial F_n}{\partial x_n} & \frac{\partial F_n}{\partial x_n} \end{bmatrix}_{\substack{\dot{x}=\dot{x}_o \\ x=x_o \\ u=u_o}} \tag{3.42}$$

$$B' = \frac{\partial F(\dot{x}_o x_o u_o)}{\partial u} = \begin{bmatrix} \frac{\partial F_1}{\partial u_1} & \frac{\partial F_1}{\partial u_2} & \frac{\partial F_1}{\partial u_n} \\ \frac{\partial F_2}{\partial u_1} & \frac{\partial F_2}{\partial u_2} & \frac{\partial F_2}{\partial u_2} \\ \frac{\partial F_n}{\partial u_n} & \frac{\partial F_n}{\partial u_n} & \frac{\partial F_n}{\partial u_n} \end{bmatrix}_{\substack{\dot{x}=\dot{x}_o \\ x=x_o \\ u=u_o}} \tag{3.43}$$

Substituting equation 3.41 to 3.43 into equation 3.39 to obtain equation 3.44

$$F(\eta) = F(\eta_o) + E(\dot{x} - \dot{x}_o) + A'(x - x_o) + B'(u - u_o) \tag{3.44}$$

If η_o is consistent with the dynamics, then, $\boldsymbol{F(\eta_o) = \bar{0}}$,

Simplifying and considering the above condition the space state model was obtained in the form;

$$\dot{x} = A\Delta x + B\Delta u \quad 3.45$$

Where;

$$A = -E^{-1}A' \quad 3.46$$

$$B = -E^{-1}B' \quad 3.47$$

9.3 Control Design

In order to correct the errors in the output of the complete aircraft model, Ziegler-Nichols heuristic PID online approach was adopted in choosing the proportional, integral and derivative gains. Firstly, a transfer function is obtained upon trimming and linearizing the aircraft model. The transfer function is further represented as the plant and the output error is corrected accordingly to enable the plant achieve its desired input. The detailed procedures adopted in the process are listed below;

1. A small proportional gain, $\boldsymbol{K_p}$ was selected and the integral and derivative gains are set to zero $\boldsymbol{K_i = K_d = 0}$. See Figure 4 below.

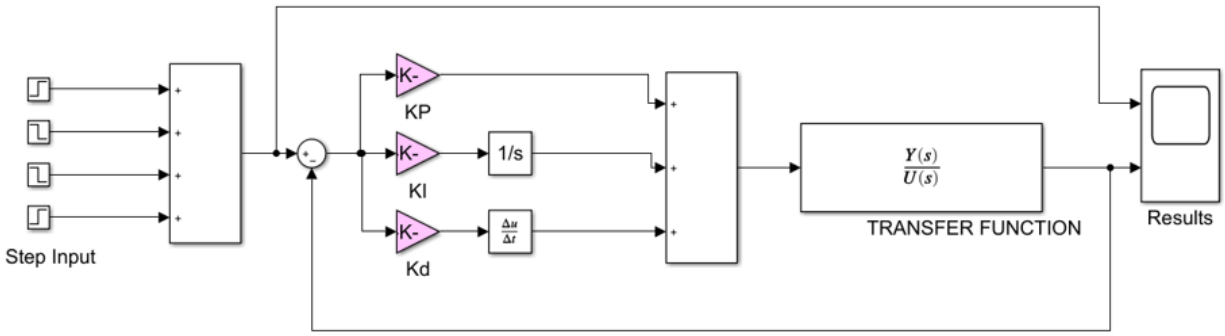

Figure 4: Selecting PID gains

2. To obtain the value of $\boldsymbol{K_p}$, the proportional gain was increased until a neutral stability was established.

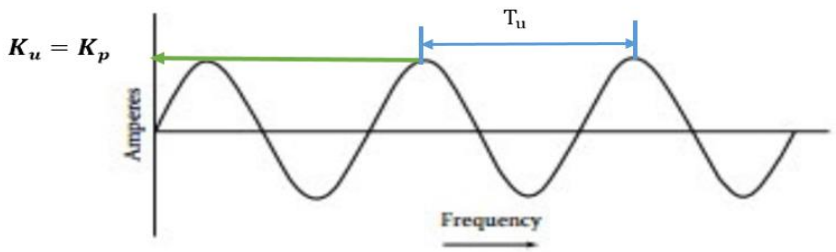

Figure 5: Neutral Stability

3. The critical/ultimate value at neutral stability was recorded as the proportion gain, $K_u = K_p$ **(see Figure 5)**

4. Critical/ultimate period of oscillation, T_u(seconds) was then measured. To obtain the corresponding integral and derivative gains. Ziegler-Nichols general equation (equation 3.49) was invoked (equation 3.39).

$$u(t) = K_p\left(e(t) + \frac{1}{T_i}\int_0^t e(\tau)d\tau + T_d\frac{de(t)}{dt}\right) \qquad 3.48$$

where,

$$K_i = \frac{K_p}{T_i} \text{ and } K_d = K_pT_d \qquad 3.39$$

5. Upon estimating K_u and T_u a control type was selected and the corresponding gains were estimated accordingly using Table 2. A Matlab code was written to estimate the gains for a specific control type (see Appendix).

Table 2: Ziegler-Nichols Control Type and Corresponding Gains

Control Type	K_p	T_i	T_d	K_i	K_d
P	$0.5K_u$	-	-	-	-
PI	$0.45K_u$	$T_u/1.2$	-	$0.54K_u/T_u$	-
PD	$0.8K_u$	-	$T_u/8$	-	$K_uT_u/10$
Classic PID	$0.6K_u$	$T_u/2$	$T_u/8$	-	$K_uT_u/10$
Pessen Integral Rule	$7K_u/10$	$2T_u/5$	$3T_u/20$	$1.75K_u/T_u$	$21K_uT_u/200$
Some Overshoot	$K_u/3$	$T_u/2$	$T_u/3$	$2/3*K_u/T_u$	$K_uT_u/9$
No Overshoot	$K_u/3$	$T_u/2$	$T_u/3$	$2/5*K_u/T_u$	$K_uT_u/15$

10. Results

10.1 Open Loop (Constant Elevator Input)

Upon initializing the aircraft model and running the simulation, the aircraft open loop results are presented in Figure 6 below. For a constant elevator input within a simulation time of 200 seconds the model produces fairly good results in both the long period and short period modes. The linear velocity components (u and w), pitch rate, pitch angle, engine speed, airpeed and angle of attack short period response last for approximately 60 seconds as opposed to the long period mode of 140 seconds. For a set throttle input of 50 % the mass flow rate decreases accordingly with instantaneous drop in aircraft's speed. The steady state for the long period lasts longer compared to the short period mode as shown in Figure 6.

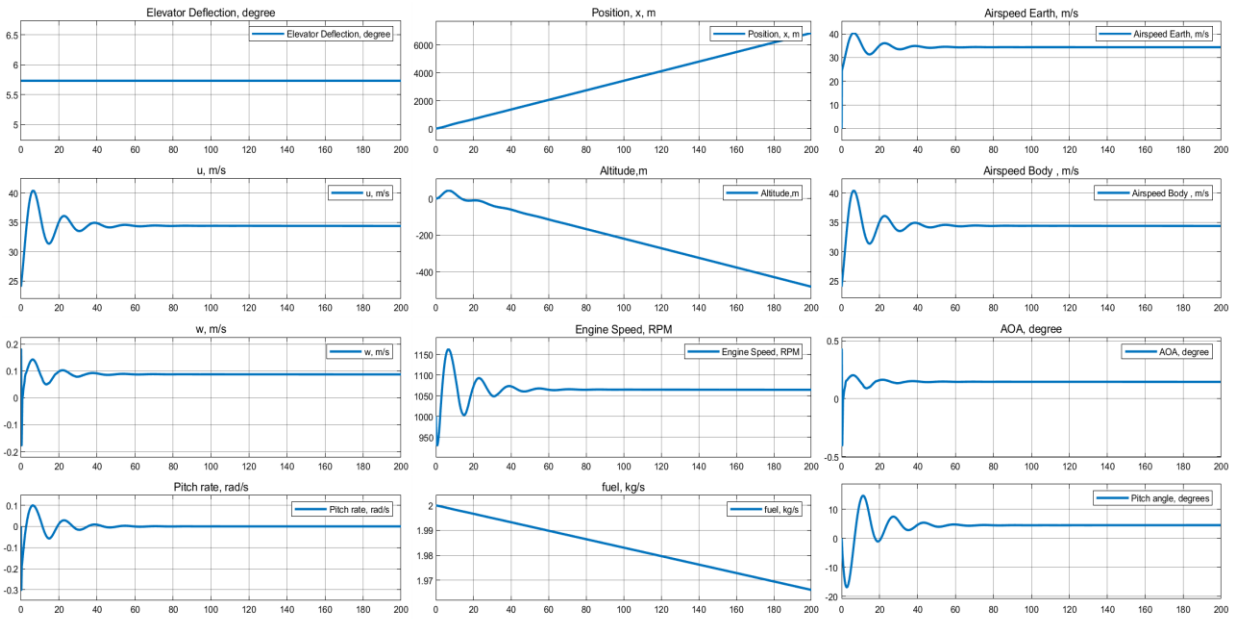

Figure 6: Open Loop Results with Constant Elevator Input

10.2 Open Loop (Constant Throttle Input)

The performance of the aircraft model was monitored for a throttle input of 50 % and varying elavator input as shown in Figure 7 below. The linear velocity components (u and w), pitch rate (q), engine speed, airpeed and angle of attack attack responds to the disturbance introduce into the aircraft model accordingly. For plus 5 and minus 5 degree elevator deflection within the periods of 40 and 100 seconds the open loop model achieves steady state at about 180 seconds.

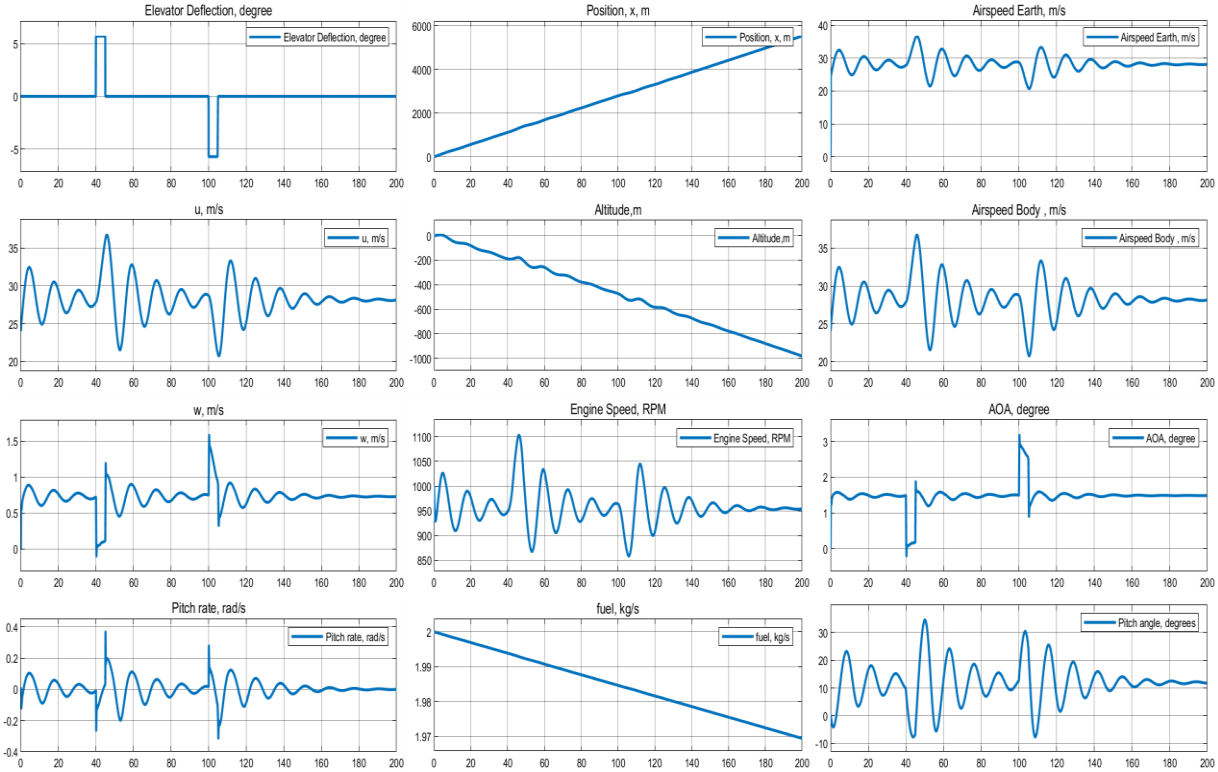

Figure 7: Open Loop Results with Varying Elevator Inputs

10.3 Trimming the Model for Steady State Level Flight

The operating points at which the aircraft model is trimmed for steady state level flight are shown in Table 3 below.

Table 3: Trimmed Inputs

INPUT	
Throttle	0.556
Elevator Deflection	0.0317 rad
OUTPUT	
Distance along, x	2000 m
Distance along z	1000 m
Velocity in x, u	33.85 m/s
Velocity in z, w	0.615 m/s
Pitch angle, theta	0.146 rad
Pitch rate, q	5.6×10^{-20} rad/s
Engine Speed	1000 RPM
Mass flow rate	2 kg/s

10.4 Trim (Operating Points) Initialization

Upon initializing the aircraft model with the trimmed operating points the model maintains a steady level flight with considerably little to no change in the primary state variable (u, w, q, θ, α). For the trimmed elevator deflection and throttle inputs the aircraft stays within the trimmed airspeed of 31 m/s and a pitch rate of about 0 rad per seconds as shown in Figure 8. The AOA stays within 0.536-0.534 for the entire simulation time.

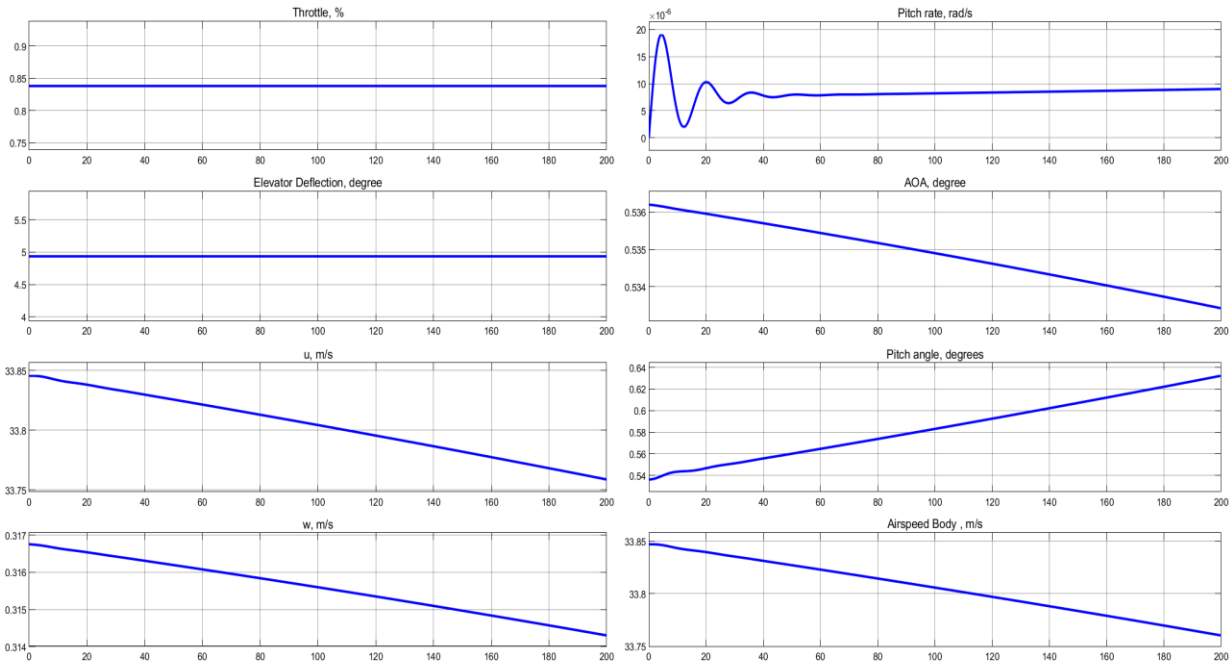

Figure 8: Trimmed Results at Constant Elevator Input

10.5 Space-State Model for Linearized aircraft

Upon numerically differentiating the elements of the Jocabian matrix and taking the input as elevator deflection and the output as the longitudinal state variables (u, w, q, h, θ), the space state model of the linearized aircraft model obtained for a given pitch rate is obtained as equation 4.1 and 4.2.

$$A = \begin{bmatrix} -0.3325 & 0.3833 & -0.6048 & 0.01296 & 0.01296 \\ -0.5242 & -5.113 & 30.34000 & 0.000 & -9.705 \\ 0.4306 & -5.373 & -5.8990 & -0.0101 & -1.431 \\ -0.1459 & 0.9893 & 0.000000 & 0.0000 & 0.00000 \\ 0 & 0 & 1.000 & 0.00000 & 0.0000 \end{bmatrix} \quad \textbf{4.1}$$

$$B = \begin{bmatrix} -0.323 \\ -3.652 \\ -49.44 \\ 0.000 \\ 0.000 \end{bmatrix} \quad \textbf{4.2}$$

10.6 Transfer Functions of the Linearized Aircraft Model

The transfer function obtained for the linearized longitudinal aircraft model outputs (q, h, V_a, AOA, θ) with respect to the elevator deflection are shown in equation 4.3 to 4.7 below. These transfer functions were used to develop PID controllers for the system.

$$\frac{\delta_q}{\delta_e} = \frac{-49.44s^6 - 391s^5 - 776.9s^4 - 131.1s^3 + 0.08024s^2 + 1.305\times10^{-6}s + 9.542\times10^{-23}}{s^7 + 14.2s^6 + 229.2s^5 + 617.9s^4 + 114.1s^3 + 114.8s^2 - 0.2148s - 3.674\times10^{-06}} \quad \textbf{4.3}$$

$$\frac{\delta_h}{\delta_e} = \frac{-3.566s^5 + 1.631s^4 + 7277s^3 + 2.287\times10^4 s^2 + 2381s - 0.004509}{s^7 + 14.2s^6 + 229.2s^5 + 617.9s^4 + 114.1s^3 + 114.8s^2 - 0.2148s - 3.674\times10^{-06}} \quad \textbf{4.4}$$

$$\frac{\delta_{Va}}{\delta_e} = \frac{-0.3953s^6 - 6.378s^5 - 48.88s^4 + 2190s^3 + 6535s^2 - 5.451s - 8.818\times10^{-5}}{s^7 + 14.2s^6 + 229.2s^5 + 617.9s^4 + 114.1s^3 + 114.8s^2 - 0.2148s - 3.674\times10^{-06}} \quad \textbf{4.5}$$

$$\frac{\delta_\theta}{\delta_e} = \frac{-49.44s^5 - 391s^4 - 776.9s^3 - 131.1s^2 + 0.08024s + 1.305\times10^{-6}}{s^7 + 14.2s^6 + 229.2s^5 + 617.9s^4 + 114.1s^3 + 114.8s^2 - 0.2148s - 3.674\times10^{-06}} \quad \textbf{4.6}$$

$$\frac{\delta_{AOA}}{\delta_e} = \frac{-0.1001s^5 - 32.85s^4 - 127.5s^3 - 27.64s^2 - 17.3s - 0.001547}{s^6 + 13.3s^5 + 164s^4 + 507.8s^3 + 114.8s^2 + 119.3s + 0.009112} \quad \textbf{4.7}$$

10.7 Pitch Rate Controller

The pitch rate controller design approach is presented in Figure 9 below. The transfer function in equation 4.3 is represented as the plant. The PID gains obtained upon using the Ziegler Nichols approach is shown in Table 4 below.

Table 4: Pitch Rate PID controller gains

Gains	Values
KP	-2.0454
KI	-0.5264

Upon implementing the gains of the PID controller the model works efficiently by allowing the system to respond to its set input. The system uses pitch rate error to generate the elevator deflection as shown in Figure 9.

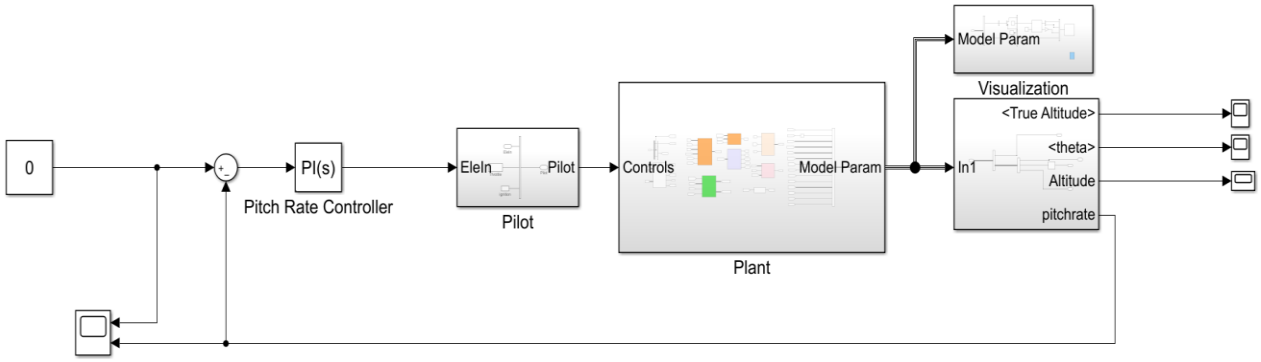

Figure 9: Pitch Rate Controller Block diagram

For a set pitch rate of 0 radians the system responded by maintaining a constant pitch rate within a period of about 80 seconds with a slight overshoot as shown in Figure 10.

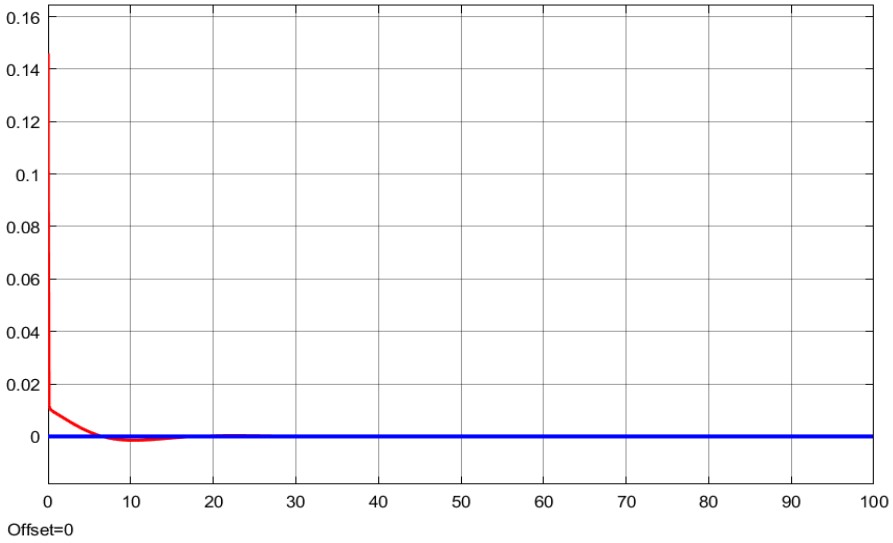

Figure 10: Pitch Rate Response on Actual Aircraft Model

10.8 Pitch Angle Controller

Using the control design technique adopted earlier, the PI gains were estimated to enable the system obtain it desired output. The transfer function in equation 4.6 is represented as the plant. The PI gains obtained are shown in Table 5 below.

Table 5: Pitch Angle Controller Gains

Gains	Values
KP	-1.44407
KI	-0.61080

For a step input with elevator deflection at times 40 and 100 seconds the system response follows the step input accordingly as shown in Figure 11 below

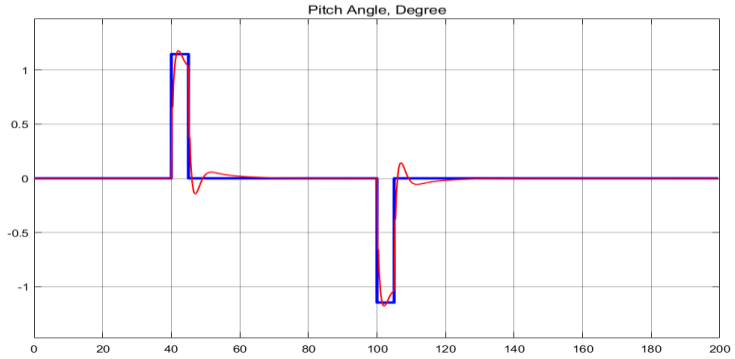

Figure 11: Pitch Angle Controller Response using Transfer Function

The model uses a traditional two-loop feedback controller to produce the desired pitch angle as shown in Figure 12. The control loop is responsible for stabilizing the pitch attitude of the system. The inner loop uses the pitch rate to enhance a stabilized pitch angle.

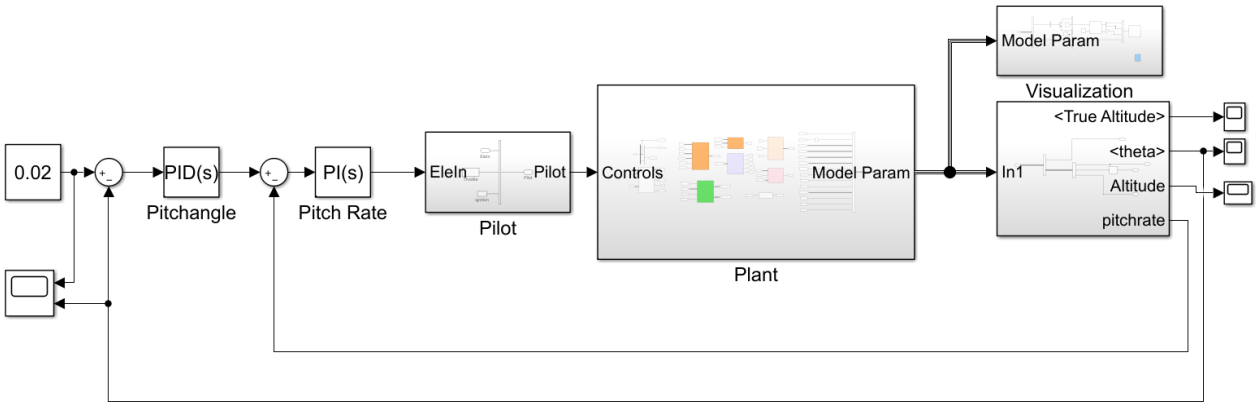

Figure 12: Pitch Angle Controller on Actual Aircraft model

For a reference pitch rate of 0.02 radians (1.15 degrees) the system responded by maintaining a constant pitch rate within a period of about 70 seconds as shown in Figure 13.

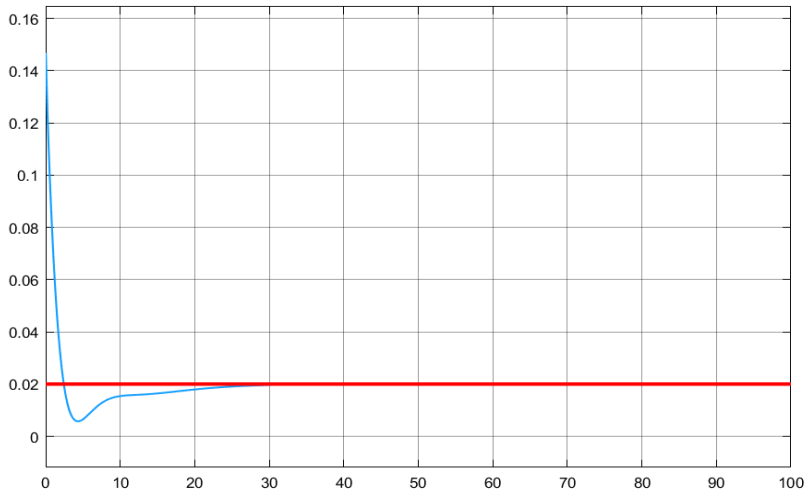

Figure 13: Pitch Angle (via Pitch Rate) Response on Actual Aircraft Model

10.9 Air Speed Controller

In a similar fashion the airspeed controller was designed using the approach aforementioned. The transfer function in equation 4.5 is represented as the plant. The PID gains obtained upon using the Ziegler Nichols approach is shown in Table 6 below.

Table 6: Airspeed Controller Gains

Gains	Values
KP	0.06070
KI	0.00818
KD	0.11239

For a step input with elevator deflection at times 40 and 100 seconds the system response follows the step input accordingly as shown in Figure 14.

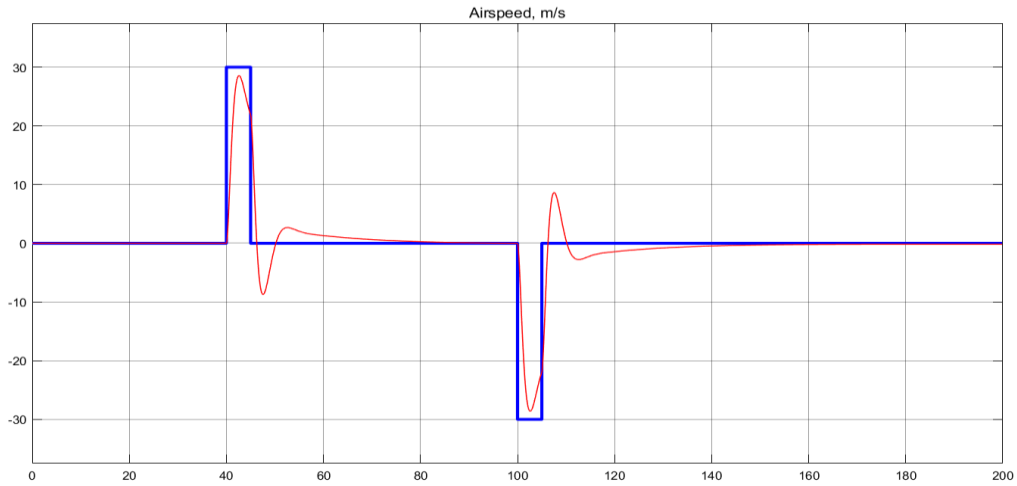

Figure 14: Airspeed Controller Response using Transfer Function

A three loop feedback controller approach was used to control the vehicle speed as indicated in Figure 15. The model uses the pitch angle and pitch rate error to command the elevator to move at a desired vehicle speed.

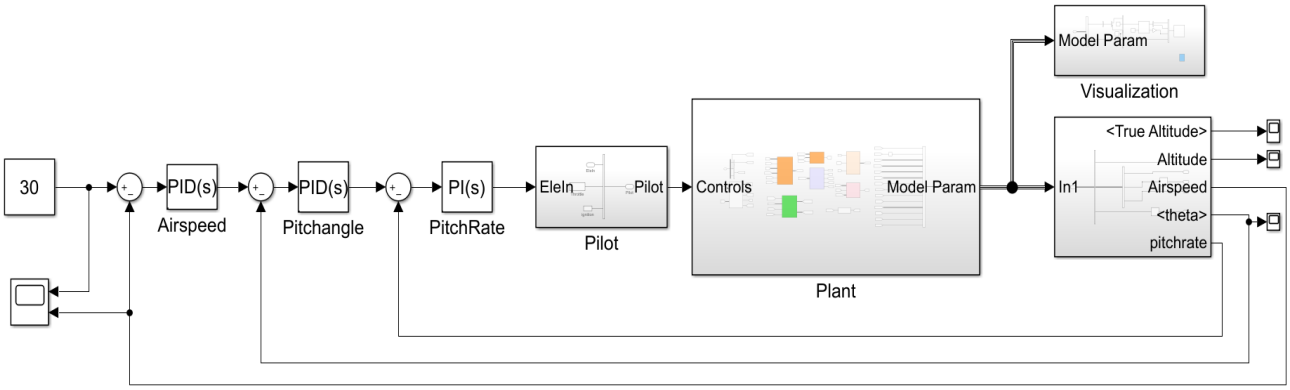

Figure 15: Airspeed Controller on Actual Aircraft Model

For a corresponding elevator and throttle input, the model produces some pitch angle that maintains the aircraft at the reference airspeed of 30 m/s as shown in Figure 16. Per the inputs defined the aircraft maintains a steady state flight in the long period mode for 80 seconds as opposed to 20 seconds short period flight time.

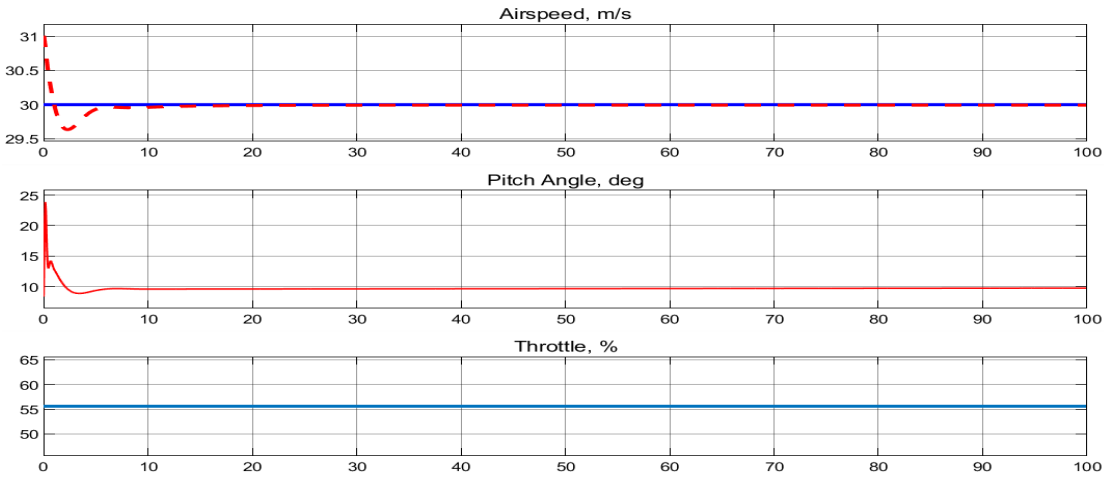

Figure 16: Airspeed Pitch Angle Controller Response

10.10 Altitude Control

To maintain the trimmed altitude at 1000 m for the entire flight simulation the pitch angle and pitch rate error, as indicated in Figure 17, were used. The model attains the reference altitude within a period of 30 seconds and maintains the reference altitude for 70 seconds. In other to further evaluate the model and the efficiency of the control scheme adapted for the altitude control the model was made to execute a set trajectory. The elevator input produces a corresponding pitch angle that enable the model perform climb, cruise and descent accordingly as shown in Figure 18. The model aggressively climbs to an altitude of 1500 m within a period of 30s and further cruise for 40s and descent to the ground within 30s.

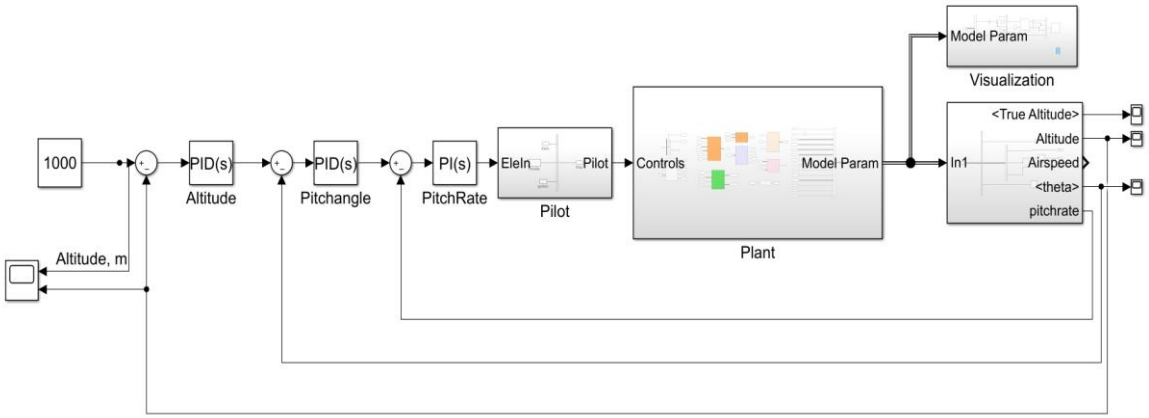

Figure 17: Altitude Control

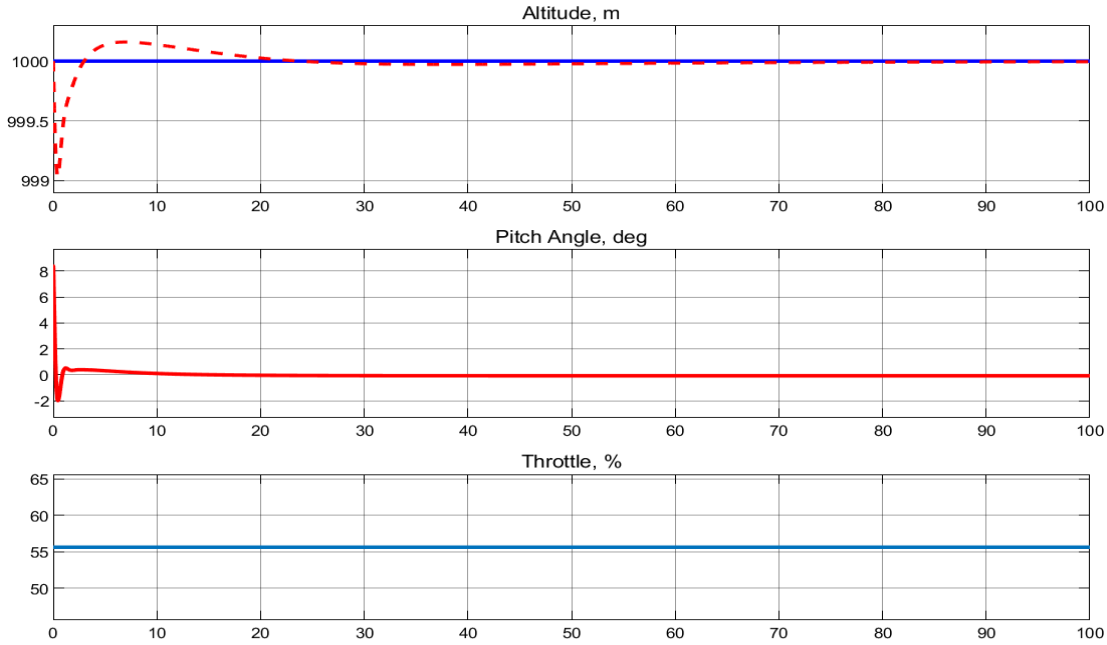

Figure 18: Altitude Controller Response

10.11 Effect of Wind on Aircraft Propulsion

The wind velocity components are shown in Figure 19 with a lot of disturbances in the velocity along the x-direction and the θ direction. With a head wind of approximately 30 m/s the performance of the engine is drastically affected. The engine power, torque, brake mean specific fuel consumption and mass flow rate requirements increase as shown in Figure 20.

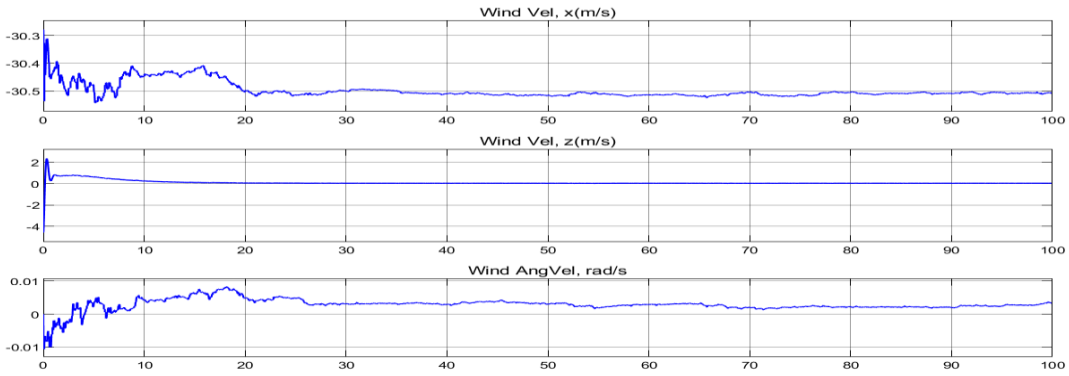

Figure 19: Wind Velocity Components

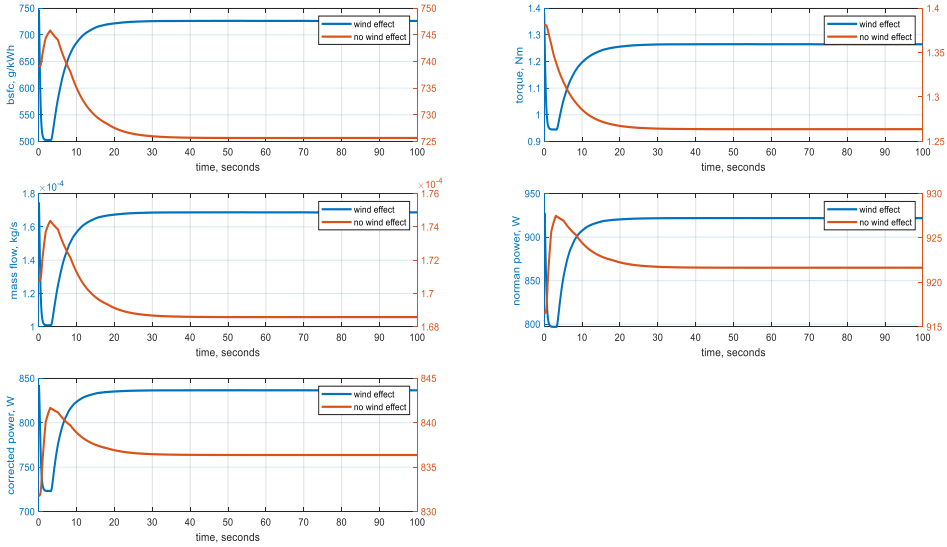

Figure 20: Effect of wind on Propulsion

11. Conclusion

A three degree of freedom aircraft model that uses the nonlinear longitudinal equation of motion to predict the states and behavior of unmanned aerial vehicle was developed. The model was successfully trimmed and the operating points obtained upon trimming is used to linearize the entire aircraft model. The Ziegler Nichol control scheme predicts the PID gains that stabilizes the aircraft in its longitudinal mode. The model accurately characterizes the behavior of the aircraft by enabling it execute a set trajectory. Dryden's wind turbulence model introduced into the equation of motion helped to quantify the effect of wind on the propulsion system used.

12. Bibliography

1. Ahmed, A. E., Hafez, A., Ouda, A. N., Ahmed, H. E. H., & Abd-elkader, H. M. (2015). Modelling of a Small Unmanned Aerial Vehicle. *Advances in Robotics & Automation*, *04*(01), 503–511. https://doi.org/10.4172/2168-9695.1000126
2. Ahmed, U. (2012). *3-DOF Longitudinal Flight Simulation Modeling And Design Using MATLAB / SIMULINK*.
3. *Construction of a Fixed-Wing Unmanned Arial Vehicle for Oil and Gas Pipeline Surveillance*. https://doi.org/10.3844/jastsp.2017.18.29
4. Raymer. (1992). *D. Raymer - Aircraft Design. A Conceptual Approach (1992).pdf*. American Institute of Aeronautics and Astrinautics.
5. Roskam, J. (1997). *[Airplane Design] Jan Roskam - Airplane Design Part II_ Preliminary Configuration Design and Integration of the Propulsion System 2(1997, DARcorporation)*. DARcorporation.
6. Sadraey, M., & Colgren, R. (2005). UAV flight simulation: Credibility of linear decoupled vs. nonlinear coupled equations of motion. *Collection of Technical Papers - AIAA Modeling and Simulation Technologies Conference 2005*, *2*(August), 1062–1076.
7. Sadraey, M., & Colgren, R. (2005). UAV flight simulation: Credibility of linear decoupled vs. nonlinear coupled equations of motion. *Collection of Technical Papers - AIAA Modeling and Simulation Technologies Conference 2005*, *2*(August), 1062–1076. https://doi.org/10.2514/6.2005-6425
8. Siradjuddin, I., Azhar, G. Al, Rahmad, C., Rohman, F., Fitriani, I. M., Pradani, E. R. K., Rohadi, E., Ronilaya, F., & Asmara, R. A. (2018). A Non-Iterative Solution for Rigid Body Transformation Estimation. *Proceedings - 2018 International Conference on Applied Science and Technology, ICAST 2018*, 573–576. https://doi.org/10.1109/iCAST1.2018.8751534
9.

13. Project Participants

Southern University:

- Dr. Stephen Akwaboa
- Mr. Amankwah Kofi Agyemang; graduated in fall 2021*

Louisiana University:

- Dr. Shyam Menon
- Mr. Darren Dehesa; graduated in fall 2021

Oregon State University:

- Dr. Chris Hagen
- Mr. James Benbrook; graduated in fall 2021

14. Publications Resulting from This Award

*Dehesa, D. A., & **Menon, S.** (2019). Modeling of Hybrid-Electric Powertrain for Unmanned Aerial Systems, AIAA Propulsion and Energy 2019 Forum, Aug.19-22, Indianapolis, IN.*

*Kofi Agyemang, **Akwaboa, S.** (2020). Three Degree of Freedom Aircraft Model for Unmanned Aerial Vehicles, ASFE, 5TH Thermal and Fluids Engineering Conference January, 5-8th April, New Orleans.*

*Benbrook, J. A., & **Hagen, C.** (2019). Hybrid Powertrain Improvements for Increased Flight Duration in Multirotor Unmanned Aerial Systems, AIAA Propulsion and Energy 2019 Forum, Aug.19-22, Indianapolis, IN.*